Life Sciences 232 (2019) 116546

Contents lists available at ScienceDirect

Life Sciences

journal homepage: www.elsevier.com/locate/lifescie

Galectin-3 aggravates pulmonary arterial hypertension *via* immunomodulation in congenital heart disease

Qiang Shen[a], Wei Chen[b,*], Jun Liu[a], Qingsong Liang[c]

[a] Department of Cardiology, University of South China Affiliated Huaihua Hospital, Huaihua 418000, PR China
[b] Department of Geriatrics Medicine, University of South China Affiliated Changsha Central Hospital, Changsha 410004, PR China
[c] Department of Neurosurgery, the Fourth People's Hospital of Huaihua, Huaihua 418000, PR China

ARTICLE INFO

Keywords:
Pulmonary arterial hypertension
Congenital heart disease
Galectin-3
T helper 2
$CD4^+T$
Pulmonary artery smooth muscle cells

ABSTRACT

Pulmonary arterial hypertension (PAH) is reported to contribute to right ventricular failure and death. PAH of variable degrees is often related to congenital heart disease (CHD). Galectin-3 (Gal-3) has been proven to be of great importance in PAH and CHD. Therefore, we investigated the specific mechanism of Gal-3 in CHD-PAH. Patients with CHD-PAH were enrolled to detect the changes of T-cell subsets, cytokine levels, and other related inflammatory cells in the plasma and to assess the Gal-3 levels in the serum. Next, CHD-PAH mouse models were established and treated with restored or depleted Gal-3 to evaluate the systolic pulmonary artery pressure (sPAP) and right ventricular hypertrophy index (RVHI), to determine levels of IL-4, IL-5, IL-13, AKT and p-AKT along with proliferation of pulmonary artery smooth muscle cells (PASMCs). Finally, we explored the effects of adoptive transfer of $CD4^+T$ cells on CHD-PAH in mice with Gal-3 knockdown to further investigate the role of Gal-3 *in vivo*. Initially, Gal-3 was up-regulated in patients with CHD-PAH. Subsequently, it was demonstrated that restored Gal-3 increased sPAP and RVHI, and promoted proliferation of PASMCs by activating the immune response with elevated levels of IL-4, IL-5, IL-13 and p-AKT. Finally, adoptive transfer of $CD4^+T$ cells promoted $CD4^+T$ cell perivascular infiltration and the progression of CHD-PAH in mice with Gal-3 knockdown. Collectively, the current study suggests a facilitating role of Gal-3 in pulmonary artery remodeling and progression of CHD-PAH *via* activation of Th2.

1. Introduction

Pulmonary arterial hypertension (PAH) is a progressive disease, featured by elevated pulmonary arterial pressure and pulmonary vascular resistance, contributing to right ventricular failure and eventually, death [1]. The pathophysiology of PAH is characterized by vascular remodeling and vasoconstrictive and proliferative thrombotic phenotype [2]. Interestingly, Lee et al. suggested that immunomodulation and inflammation are implicated in patients suffering from PAH [3]. Unfortunately, the morbidity and mortality of PAH continue to grow [4]. Although progresses have been made regarding the treatment in recent years, only a few treatment modalities can be used to treat PAH [5]. Pulmonary hypertension (PH) is a prevalent complication that negatively affects the survival and functional capacity of patients with congenital heart disease (CHD) [6]. About 5% - 10% of patients with CHD suffer from PAH of varying degrees [7]. Reportedly, there are 400–500 individuals suffering from PAH in every 5500 patients with CHD, with the shunt-related PAH being the most universal subtype [8]. Although there are some improvements in treatment for PAH-CHD, the specific mechanisms for PAH-CHD, such as treatment targets, remain unclear [9]. Therefore, it is necessary to elucidate the specific mechanism for PAH-CHD for effective therapeutic targets for PAH-CHD.

Galectin-3 (Gal-3), a member of β-galactoside binding lectin family, is commonly expressed in the nucleus, cell surface, and extracellular space [10]. Also expressed in inflammatory cells, fibroblasts, and myocardium, Gal-3 has been demonstrated to participate in most models of injury [11]. Accordingly, Gal-3 is already established as a biomarker for cardiac fibrosis, and chronic left ventricular heart failure [12]. Gal-3, as a prognostic biomarker for PAH, affects the progression of PAH by regulating important processes such as proliferation and differentiation [13]. Moreover, Calvier et al. confirmed that silencing of Gal-3 serves as a potential target for hypoxia-induced PAH treatment [14]. Furthermore, Gal-3 also exerts significant effects on the functional capacity, cardiac function and adverse cardiovascular events in adult

* Corresponding author at: Department of Geriatrics Medicine, University of South China Affiliated Changsha Central Hospital, No. 161, Shaoshan South Road, Yuhua District, Changsha 410004, Hunan Province, PR China.
E-mail address: 18974579899@189.cn (W. Chen).

https://doi.org/10.1016/j.lfs.2019.116546
Received 22 February 2019; Received in revised form 24 May 2019; Accepted 5 June 2019
Available online 06 June 2019

patients with CHD [15]. Hence, we proposed a hypothesis that Gal-3 might play a critical role in CHD-related PAH. Accordingly, the current study enrolled patients and established CHD-PAH mouse models to explore the specific mechanism of Gal-3 in CHD-PAH by affecting the immune response.

2. Materials and methods

2.1. Ethics statement

The current study was carried out with the approval of the Ethics Committee of University of South China Affiliated Huaihua Hospital. Signed informed consents were obtained from all participants. Additionally, the animal experiment procedures were conducted according to the protocols approved by the Institutional Animal Research Committee of University of South China Affiliated Huaihua Hospital.

2.2. Study subjects

A total of 42 patients diagnosed as CHD-PAH at the Department of Cardiology, University of South China Affiliated Huaihua Hospital and Department of Geriatrics Medicine, University of South China Affiliated Changsha Central Hospital between April 2013 and June 2014 were included in the current study. Among the enrolled patients, there were 10 males and 32 females, and the calculated median age was 34.9 years, ranging from 18 to 66 years. There were 29 cases of atrial septal defects (ASDs), 9 cases of ventricular septal defects (VSDs), and 4 cases of patent ductus arteriosus (PDA). In addition, 20 healthy subjects (5 males and 15 females) with matching age and gender in physical examination center of University of South China Affiliated Huaihua Hospital were enrolled in the study. The classification of cardiac function of all patients ranged from grade I to grade III. All patients received no targeted drugs for PAH or drugs for improving right ventricular function. PAH patients presenting with acute myocardial infarction, unstable angina pectoris, hepatic insufficiency, and renal insufficiency, or patients with PAH caused by other reasons were excluded. All participants underwent 6-minute walk tests, and 4 mL venous blood samples were extracted from the femoral vein and stored in anticoagulant and procoagulant tubes when the participants were undergoing treatment with occlusion operation in catheter room or right cardiac catheterization, respectively. Next, the samples were centrifuged for 5 min for extraction of upper plasma or serum which was placed in an Eppendorf tube and preserved at −80 °C.

2.3. Experimental animals

A total of 108 BALB/C male mice (weighing 20–30 g) with specific pathogen-free grade were purchase from Hunan SJA Laboratory Animal Co., Ltd. (Changsha, Hunan, China). All mice were raised in cages (5 mice in each cage) at 21 °C with relative humidity of 50% - 80%, 12 h day/night cycle, and free access to food and water. The mice were used to establish CHD-PAH mouse models (n = 104), treated with sham operation (n = 12), and received no treatment (n = 12) [8].

2.4. Establishment of mouse models

The BALB/C mice (aged 4 weeks) were weighed and intraperitoneally anesthetized with 1% sodium pentobarbital (80 mg/kg). Next, the abdominal aorta and inferior vena cava were exposed. A transverse incision was made using micro-scissors with a curved tip in the anterior wall of the abdominal aorta to expose the contralateral wall. The contralateral wall was adjacent to the wall of the inferior vena cava. After the shunt was made, the incision in the abdominal aorta wall was sutured using 11-0 polypropylene monofilament. Then, the blocking flament was loosened, and the inferior vena cava pulsed and was swollen with arterial blood, which indicated the presence of a shunt. The mice treated with sham operation did not have an arteriovenous shunt. After the incision, anterior wall of the abdominal aorta was sutured immediately [8].

The CHD-PAH mouse models were treated with a single tail vein injection of 100 μL lentivirus vectors (5×10^7 TU/mL, Shanghai Genechem Co., Ltd. (Shanghai, China) containing sh-negative control (NC), sh-GAL-3, oe-NC or oe-GAL-3 and $CD4^+$T) at day 0 after establishment, with 12 mice for each treatment [16–18]. The $CD4^+$ cells were separated and purified from the spleen of mice using magnetic cell sorting. The adoptive transfer was conducted according to previous literature and guidelines [19]. A total of 4×10^6 cells were injected into the mice treated with shunt, sh-GAL-3 and $CD4^+$T.

2.5. Evaluation of the pulmonary artery pressure (PAP)

The mice were treated with direct intubation anesthesia and the cannula was directly introduced into the trachea. The parameters of small animal ventilator were set to 120 beats/min as frequency, 0.15 mL (6–8 mL/kg) as tidal volume, and inhaled oxygen concentration of 21%. A polyethylene catheter full of heparin solution was connected to one end of the pressure transducer to record the pressure curve, while the other end was connected to a 27-G needle, which was punctured into the right ventricle along the right ventricular outflow. When the pressure waveform was observed to be stable, data were recorded. The systolic pulmonary artery pressure (sPAP) was represented by right ventricular systolic pressure, which was evaluated at the 4th, 6th, 8th, and 12th weeks after operation [8].

2.6. Evaluation of the right ventricular hypertrophy index (RVHI)

The right ventricular outflow was punctured using a needle in order to infuse the lungs with saline, and eventually the lungs turned completely white. The atrium and major vessel roots were incised. Next, the right ventricular wall was isolated along the groove of the posterior ventricle. A precision electronic scale was employed to weigh the right ventricular free wall (RV) and the left ventricle free wall plus the septum (LV + S). RV/LV + S was used to calculate RVHI at the 12th week [8].

2.7. Hematoxylin and eosin (HE) staining

At least 5 small muscular arteries with complete internal and external elastic lamina were randomly selected from the lung tissue sections, and stained with HE for visualization. The inner and outer elastic lamina contours were outlined using the cursor within an Axioplan 2 microscope imaging analysis system (Carl Zeiss MicroImaging, Inc., Thornwood, NY, USA) to assess the medial thickness (MT), external diameter (ED), and internal diameter (ID). The mean medial thickness percentage (MT%) was calculated using the following formula: $MT\% = (2 \times MT \div ED) \times 100$ [8,20].

2.8. Immunofluorescence assay

Lung tissue sections of mice were fixed in the cold acetone (5 μm) and rinsed with phosphate-buffered saline (PBS) (0.15 M, pH = 7.4). The samples were permeated using PBS supplemented with 0.25% Triton X-100 for 10 min, followed by incubation with 3% bovine serum albumin (BSA)/PBS for 0.5–1 h to block the nonspecific binding of antibody. Subsequently, the samples were incubated with specific primary mouse antibody to α-smooth muscle actin (α-SMA) (dilution ratio of 1:500; Sigma-Aldrich Chemical Company, St Louis, MO, USA) and CD4 (dilution ratio of 1:50; eBioscience, San Diego, CA, USA) at 4 °C overnight. After that, the samples were incubated with the secondary antibody coupling with Alexa Fluor 488, Alexa Fluor 594, or Alexa Fluor 633 (Invitrogen, Carlsbad, CA, USA) for 1–2 h. The sections were then fixed and stained with prolonged gold anti-fading reagent and 4′,

6-diamidino-2-phenylindole (DAPI) (Invitrogen, Carlsbad, CA, USA).

Next, the cell slides on the plates were fixed in 4% paraformaldehyde for 15 min, and cleared with 0.5% Triton X-100 (prepared with PBS) for 20 min. Afterwards, the slides were blocked with normal goat serum at room temperature for 30 min. Then, each slide was incubated with sufficient diluted primary antibody to α-SMA (dilution ratio of 1:500; Sigma-Aldrich Chemical Company, St Louis, MO, USA) and proliferating cell nuclear antigen (PCNA) (dilution ratio of 1:1000; Cell Signaling Technology, Beverly, MA, USA) at 4 °C overnight, and further cultured with fluorescence secondary antibodies at 37 °C for 1 h. Finally, the cells were incubated with DAPI avoiding exposure to light for 5 min for nucleus staining.

All fluorescence images were observed and photographed under the laser scanning confocal microscope (Olympus, Tokyo, Japan) and analyzed using Image J (National Institutes of Health, Bethesda, Maryland, USA) or Image Pro Plus software (Media Cybernetics, Silver Springs, MD, USA) [8,21].

2.9. Enzyme-linked immunosorbent assay (ELISA)

Cytokine levels in serum, bronchoalveolar lavage fluid (BALF) supernatants, and cell culture medium were determined according to the instructions (R&D Systems, Minneapolis, MN, USA) [21]. In addition, the concentration of Gal-3 in the serum was assayed using an ELISA kit (Shanghai MEIXUAN Biological Science and Technology Co., Ltd., Shanghai, China).

2.10. Flow cytometry

A BD flow cytometer (FACScan; BD Biosciences, Franklin Lakes, NJ, USA) was employed to analyze the peripheral blood mononuclear cells (PBMCs) isolated from human blood and white blood cells from mice lung tissues. Briefly, the obtained cells were incubated in PBS containing the primary antibody and 1% BSA on ice for 30 min. The human body samples were incubated with primary antibodies to fluorescein isothiocyanate (FITC)-CD3 (dilution ratio of 1:100; Miltenyi biotec, Bergisch Gladbach, Germany), phycoerythrin (PE)-CD4 (dilution ratio of 1:100; Miltenyi biotec, Bergisch Gladbach, Germany), FITC-CD4 (dilution ratio of 1:500; eBioscience, CA, USA), PE/Cy7-CD4 (dilution ratio of 1:200; eBioscience, CA, USA), allophycocyanin (APC)-CD8 (dilution ratio of 1:100; Miltenyi biotec, Bergisch Gladbach, Germany), APC/Cy7-CCR3 (dilution ratio of 1:200; BioLegend, San Diego, CA, USA), FITC-CD123 (dilution ratio of 1:200; BioLegend, San Diego, CA, USA), Brilliant Violet 421-CD49d (dilution ratio of 1:200; BioLegend, San Diego, CA, USA), APC-HLA-DR (dilution ratio of 1:200; BioLegend, San Diego, CA, USA), APC-c-kit (dilution ratio of 1:200; BioLegend, San Diego, CA, USA), PE-FcεRIα (dilution ratio of 1:200; eBioscience, CA, USA), eFluor 450-CD127 (dilution ratio of 1:200; BioLegend, San Diego, CA, USA), FITC-CD19 (dilution ratio of 1:200; Biolegend, San Diego, CA, USA), eFluor450-B220 (dilution ratio of 1:200; eBioscience, CA, USA), PE/Cy7-IgE (dilution ratio of 1:200; Biolegend, San Diego, CA, USA), APC-CD25 (dilution ratio of 1:200; Biolegend, San Diego, CA, USA), and PE-Foxp3 (dilution ratio of 1:200; eBioscience, CA, USA). The mouse samples were cultured with the primary antibodies (eBioscience, CA, USA) to eFluor 450-CD3 (dilution ratio of 1:500), FITC-CD4 (dilution ratio of 1:500), PE/Cy7-CD4 (dilution ratio of 1:200) and PE-CD8 (1:500). Subsequently, the cells were tested using the FuffyJo8.3.3 software (Tree Star Inc., Ashland, OR, USA).

2.11. RNA isolation and quantitation

Total RNA content was extracted from the $CD4^+$T cells using a RNeasy Mini kit (Qiagen Company, Hilden, Germany). Next, the obtained RNA (1 μg) was reverse-transcribed into cDNA according to the instructions of Reverse Transcription Reagent kits (Takara Bio Inc., Otsu, Shiga, Japan). A PrimeScript RT-PCR kit (Takara Bio Inc., Otsu, Shiga, Japan) was employed to assay the Gal-3 expression with glyceraldehyde-3-phosphate dehydrogenase (GAPDH) as the internal reference. The primer sequences of Gal-3 were Forward: TTGAAGCTGA CCACTTCAAGGTT and Reverse: AGGTTCTTCATCCGATGGTTGT while those of GAPDH were Forward: ATGGAGAAGGCTGGGGCTC and Reverse: AAGTTGTCATGGATGACCTTG [14]. The relative expression levels of target genes were calculated using the $2^{-\Delta\Delta Ct}$ method. The experiment was repeated three times.

2.12. Western blot analysis

Total protein was extracted from the cells and the concentration of protein was determined with reference to the manufacturer's instructions of a bicinchoninic acid kit (Boster Biological Technology Co., Ltd., Wuhan, Hubei, China). The protein was then separated using 10% polyacrylamide gel (Boster Biological Technology Co., Ltd., Wuhan, Hubei, China) and transferred onto a polyvinylidene fluoride membrane. The membrane was blocked in 5% BSA at room temperature for 1 h, incubated with rabbit antibodies to AKT (ab64148, dilution ratio of 1:500), p-AKT (ab38449, dilution ratio of 1:1000) and β-actin (ab8227, dilution ratio of 1:2000) at 4 °C overnight and further incubated with the secondary goat anti-mouse antibody (ab6721, dilution ratio of 1:2000) at room temperature for 1 h, followed by development using chemiluminescence reagent. All aforementioned antibodies were purchased from Abcam Inc., (Cambridge, MA, USA). β-actin was used as an internal control.

2.13. Cell culture

The mice (aged 6 weeks) were euthanized by CO_2 overexposure. Proximal PAs were aseptically isolated from the lung lobe and placed in Dulbecco modified Eagle medium (DMEM) (Gibco, Carlsbad, CA, USA). After removal of adhering fat, connective tissues, and endothelial cells, the dissected medium of the PAs was then sliced into small blocks ($1–2\ mm^2$) and covered by autoclaved glass coverslips in cell culture dishes. The primary pulmonary artery smooth muscle cells (PASMCs) from mice were incubated in DMEM/F-12 (Gibco, Carlsbad, CA, USA) supplemented with 20% fetal bovine serum, 2 mM L-glutamine, 100 U/mL penicillin, and 0.1 mg/mL streptomycin. The PASMCs were identified using positive immunostaining with antibodies against α-SMA (Sigma-Aldrich Chemical Company, St Louis, MO, USA). The cells at passage 3–6 were used for further experimentation. For hypoxic exposure, PASMCs were inoculated in culture dishes and placed in a hermetic tank with 1% O_2/5% CO_2.

Purified $CD4^+$T cells were isolated from the spleens of 6–8 week-old mice using a magnetic-activated cell sorting kit (STEMCELL Technologies, Vancouver, BC, Canada). $CD4^+$T cells were induced into Th2 cells *in vitro* [22]. The Gal-3 over-expression vectors were provided by Sigma-Aldrich (St. Louis, MO, USA), and pcDNA vectors were used as negative control (NC). Th2 cells were transfected with Gal-3 over-expression vectors (50 ng pcDNAs) according to the instructions of Lipofectamine 3000 Reagent (Thermo Fisher Scientific, Rockford, IL, USA). PASMCs were co-cultured with Th2 cells by adding culture dishes with Th2 cells. The proliferation of PASMCs was detected by cell counting kit-8 (CCK-8; Dojindo Laboratories, Kumamoto, Japan) according to the instructions.

2.14. Statistical analysis

Statistical analyses were performed using the SPSS 21.0 software (IBM Corp. Armonk, NY, USA), and the measurement data with normal distribution were expressed as mean ± standard deviation. Comparisons among multiple groups were tested by one-way analysis of variance (ANOVA), and comparisons among data at different point times were tested using repeated measures ANOVA, followed by the Tukey's post-hoc test. Pairwise comparison within one group was

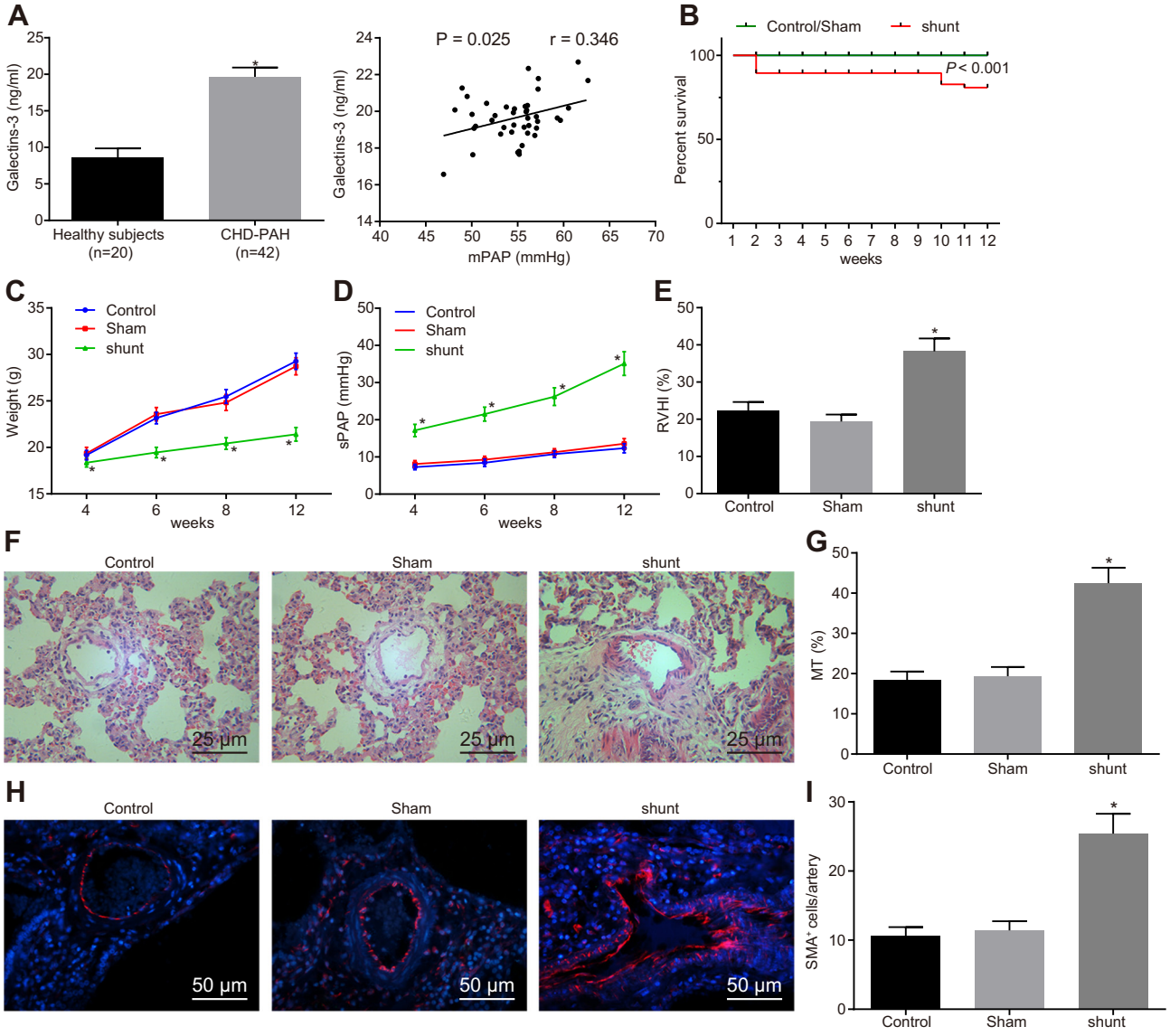

Fig. 1. High expression of Gal-3 is identified in serum of patients with CHD-PAH and the CHD-PAH mouse models were successfully established. A, Gal-3 levels in CHD-PAH patients and healthy subjects determined using ELISA. $^{**}p < 0.01$ *vs.* healthy subjects. Comparisons between CHD-PAH patients and healthy subjects were analyzed by non-paired *t*-test. B, Survival analysis of mice. C, Mouse weight after modeling. D, sPAP of mice after modeling. E, RVHI of mice at the 12th week after modeling. F, Pulmonary vascular remodeling observed using HE staining (×400). G, MT of pulmonary vascular wall in mice at the 12th week. H, immunofluorescence staining of α-SMA in lung tissue sections (×200). I, SMCs in pulmonary artery. $^{*}p < 0.05$ *vs.* the sham group (mice treated with sham operation). Data were depicted as mean ± standard deviation. Comparisons at different point times were analyzed using repeated measures ANOVA, and comparisons among multiple groups were tested by one-way ANOVA (Tukey's *post hoc* test). n = 12.

conducted using the non-paired *t*-test. Enumeration data were represented as percentage or constituent ratio, and analyzed using Fisher's precision inspection. Pearson correlation analysis was performed to analyze the relationship between X and Y. A value of $p < 0.05$ was considered to be statistically significant.

3. Results

3.1. Gal-3 is highly expressed in CHD-PAH

Gal-3, a member of the lectin family, is expressed in multiple cells and tissues, and known to play a critical role in the immune reaction [23]. We employed ELISA to determine the levels of Gal-3 in patients with CHD-PAH and healthy subjects, and the results indicated that CHD-PAH patients presented with elevated Gal-3 levels (Fig. 1A). The correlation analysis displayed that Gal-3 levels were positively related to mPAP in the serum of patients with CHD-PAH ($\gamma = 0.346$, $p = 0.025$). Thus, we speculated that Gal-3 greatly influences the progression of CHD-PAH. To explore the effects of Gal-3 on PAH, we established mice models of CHD-PAH. Next, it was identified whether mice treated with shunt could be used for investigating CHD-PAH. The findings showed that shunt mouse models exhibited increased mortality ($p = 0.025$; Fig. 1B). In addition, at the 4th week, the weight of mice in each group were found to display no significant differences, while during the 4th – 8th week, shunt mouse models showed obviously decreased weight values (Fig. 1C). Mice treated with sham operation or without treatment presented with no evident differences in mortality and weight (Fig. 1B–C). Moreover, shunt mouse models presented with increased sPAP and RVHI in comparison to mice treated with sham operation or without treatment (Fig. 1D–E). Meanwhile, at the 12th week, HE staining revealed the presence of more VSMCs and increased MT of pulmonary vascular wall in mice in shunt mouse models

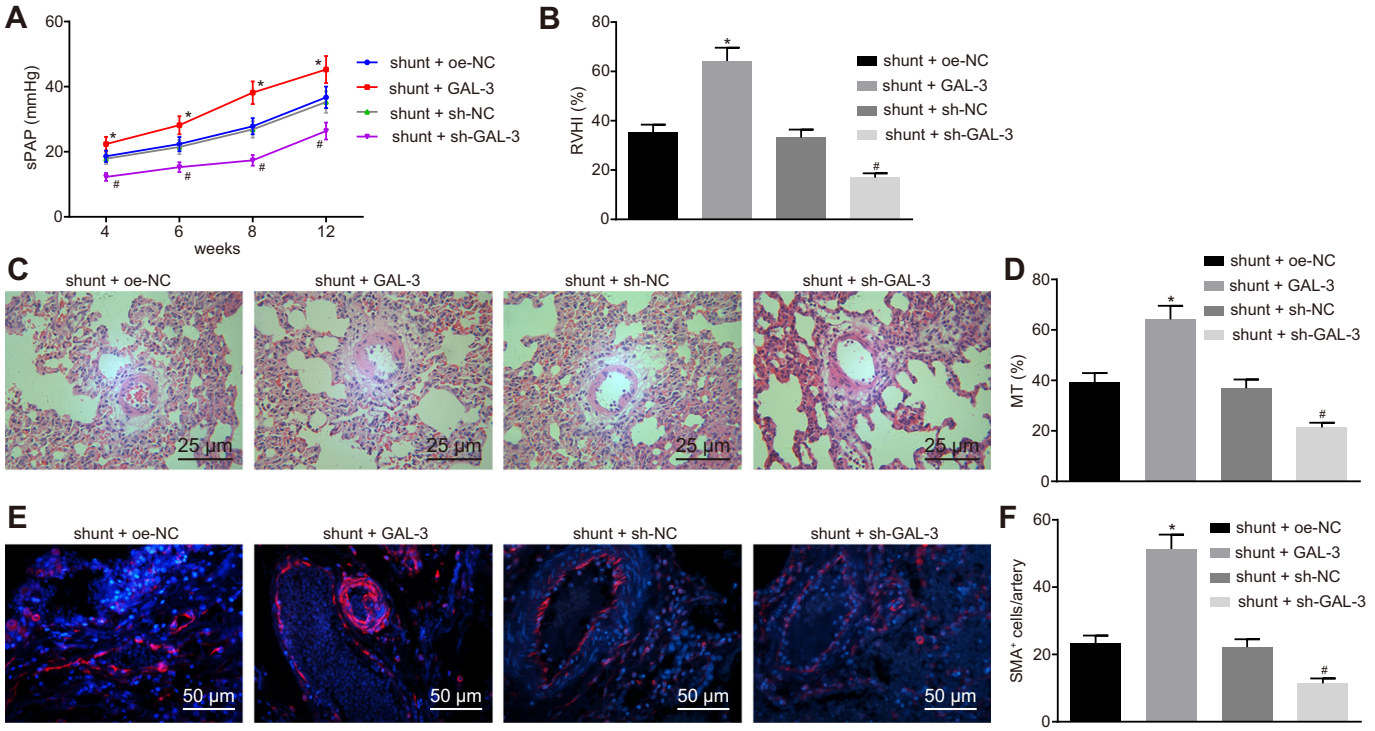

Fig. 2. Gal-3 promotes the progression of CHD-PAH in mice. A, sPAP of mice after treated with Gal-3 over-expression or depletion. B, RVHI of mice after treated with Gal-3 over-expression or depletion at the 12th week. C, Pulmonary vascular remodeling after treated with Gal-3 over-expression or depletion observed using HE staining (×400). D, MT of pulmonary vascular wall in mice after treated with Gal-3 over-expression or depletion at the 12th week. E, Immunofluorescence staining of α-SMA in lung tissue sections after treated with Gal-3 over-expression or depletion (×200). F, SMCs in pulmonary artery after treated with Gal-3 over-expression or depletion. *$p < 0.05$ *vs.* the shunt + oe-NC group (CHD-PAH mouse models treated with oe-NC plasmids), #$p < 0.05$ *vs.* the shunt + sh-NC group (CHD-PAH mouse models treated with sh-NC plasmids). Data were depicted as mean ± standard deviation. Comparisons between two groups were analyzed using non-paired *t*-test, comparisons among multiple groups were tested by one-way ANOVA (Tukey's *post hoc* test), and comparisons at different point times were analyzed using repeated measures ANOVA (Tukey's *post hoc* test). Pearson correlation analysis was also conducted. n = 12.

(Fig. 1F–G), which was further verified by means of immunofluorescence assay (Fig. 1H–I). These results demonstrated that the CHD-PAH mouse models were successfully established wherein Gal-3 was highly expressed.

3.2. Gal-3 aggravates the progression of CHD-PAH in mice

Subsequently, the CHD-PAH mouse models were treated with over-expression or silencing of Gal-3. It showed that sPAP and RVHI were significantly increased in CHD-PAH mouse models treated with Gal-3 over-expression, while obviously reduced levels were noted in CHD-PAH mouse models treated with Gal-3 knockdown (Fig. 2A–B). In addition, CHD-PAH mouse models treated with Gal-3 over-expression showed increased VSMCs and MT of the pulmonary vascular wall, while opposite results were observed in CHD-PAH mouse models treated with Gal-3 knockdown (Fig. 2C–D), which was further verified using immunofluorescence assay (Fig. 2E–F). Overall, these findings suggested that Gal-3 could aggravate the progression of CHD-PAH in mice.

3.3. Gal-3 promotes immune response in CHD-PAH mice

Previous evidences have highlighted that inflammation and autoimmunity are key factors that affect the progression of PAH [24]. Thus, we first collected PBMCs from patients with CHD-PAH and healthy subjects to detect T-cell subsets using flow cytometry. We noted that the proportion of $CD3^+CD4^+$ cells in PBMCs of patients with CHD-PAH was significantly higher than that in the healthy subjects (Table 1). However, no differences were observed among the Cytotoxic T cell ratio ($CD3^+CD8^+$ cells) (Table 1). Additionally, the levels of IL-4, IL-5, and IL-13 in peripheral blood of patients with CHD-PAH were found to be

Table 1
Clinical features in CHD-PAH patients and healthy subjects.

Parameter	CHD-PAH	Healthy subjects	*p*
General information	(n = 42)	(n = 20)	
Male/female (number)	10/32	5/15	0.459
Age (year)	35.24 ± 3.02	35.05 ± 4.45	0.845
BMI (kg/m^2)	19.36 ± 1.87	19.87 ± 1.93	0.324
Heart rate (beat/min)	83.24 ± 2.35	82.90 ± 2.47	0.624
mPAP (mmHg)	54.78 ± 3.53	–	–
6MWD (m)	355.15 ± 39.76	486.39 ± 71.12	< 0.001
Proteins			
IL-4 (pg/mL)	312.14 ± 23.57	162.14 ± 13.98	< 0.001
IL-5 (pg/mL)	221.32 ± 13.34	121.32 ± 8.37	< 0.001
IL-13 (pg/mL)	249.23 ± 13.68	109.22 ± 11.94	< 0.001
IgE (ng/mL)	210.45 ± 13.17	61.44 ± 11.32	< 0.001
Blood cells (%)			
$CD4^+$ cells	31.97 ± 1.83	19.16 ± 1.73	< 0.001
$CD8^+$ cells	15.05 ± 1.18	14.96 ± 1.38	0.002
Eosinophil	3.22 ± 0.36	2.14 ± 0.53	< 0.001
Basophil	8.75 ± 1.54	6.32 ± 0.35	< 0.001
B cell	3.92 ± 0.86	1.12 ± 0.25	< 0.001
T reg	2.12 ± 0.57	6.38 ± 0.79	< 0.001

Notes: BMI, body mass index; mPAP, mean pulmonary arterial pressure; 6MWD, 6-minute walking distance. Levels of serum cytokines and IgE in human subjects were evaluated by ELISA. Inflammatory cells in peripheral blood of human subjects were analyzed by flow cytometry. Numeration data were represented as percentage or constituent ratio, and analyzed using Fisher's precision inspection. Measurement data were depicted as mean ± standard deviation. Comparisons between two groups were analyzed using non-paired *t*-test.

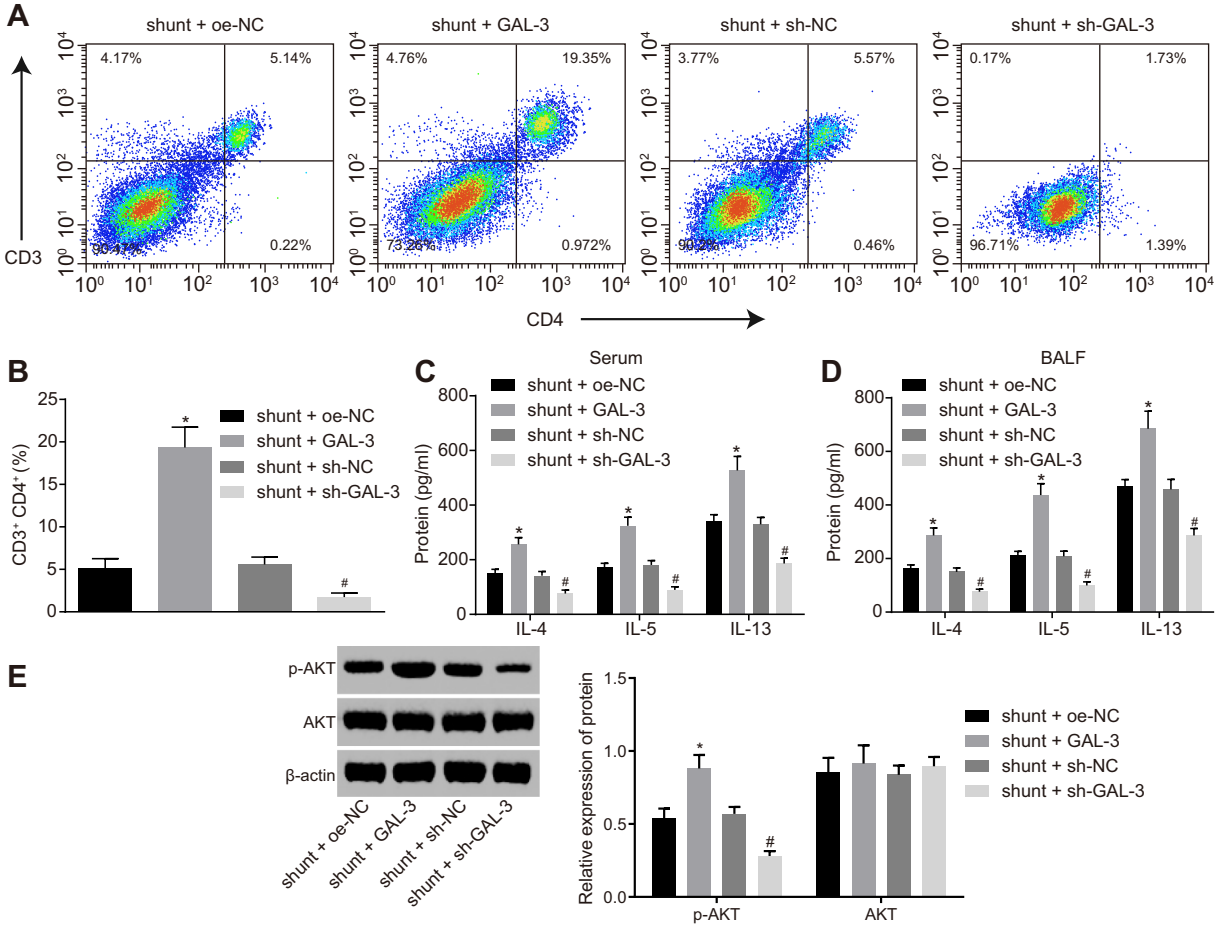

Fig. 3. Gal-3 enhances the immune response in CHD-PAH mice. A, $CD3^+CD4^+$T cells in lung tissues detected using flow cytometry. B, Percentage of $CD3^+CD4^+$T cells in lung tissues. C, Levels of IL-4, IL-5, and IL-13 in the serum determined using ELISA. D, Levels of IL-4, IL-5, and IL-13 in the BALF determined using ELISA. E, Relative protein levels of AKT and p-AKT in BALF normalized to β-actin determined by Western blot analysis. $*p < 0.05$ *vs.* the shunt + oe-NC group (CHD-PAH mouse models treated with oe-NC plasmids), $\#p < 0.05$ *vs.* the shunt + sh-NC group (CHD-PAH mouse models treated with sh-NC plasmids). Data were depicted as mean ± standard deviation. Comparisons between two groups were analyzed using non-paired *t*-test.

higher than those in the healthy subjects (Table 1). Correspondingly, major effector cells of Th2 cells, such as Eosinophil and B cells secreted by IgE, were markedly elevated in peripheral blood of patients with CHD-PAH, while T reg proportion was decreased evidently (Table 1). In order to explore whether the facilitating roles of Gal-3 in the progression of CHD-PAH was associated with T cell activation, we further studied the CHD-PAH mice using treatments for restoration or depletion of Gal-3. The findings revealed that mice treated with restored Gal-3 presented with elevated percentages of $CD3^+CD4^+$T cells and secretion of Th2 cytokines (IL-4, IL-5, and IL-13) from serum and BALF of mice, while mice treated with depleted Gal-3 displayed the opposite trends (Fig. 3A–D). Therefore, the obtained data suggested that Gal-3 could promote the immune response in CHD-PAH mice.

In addition, the AKT signaling pathway has been indicated to be of great importance in the occurrence of PAH [25–27]. However, the regulatory role of Gal-3 on the AKT signaling pathway still remains to be explored. Herein, it was conjectured that the effects of Gal-3 on PAH might be achieved through the AKT signaling pathway. The activation of the AKT signaling pathway was detected by means of Western blot analysis. Results showed that treatment of shunt + GAL-3 exerted no significant effects on the protein levels of AKT but increased the extent of AKT phosphorylation, while treatment of shunt + sh-GAL-3 induced opposite trends (Fig. 3E). Taken together, it could be inferred that the AKT signaling pathway plays a role in the effects of Gal-3 on CHD-PAH.

3.4. Gal-3 promotes proliferation of PASMCs by activating immune response

After verification of the role of Gal-3 in immune response in CHD-PAH mice, the focus of the current study was further shifted to elucidating the mechanisms of Gal-3 in proliferation of PASMCs. A co-culture system with anoxic environment (1% O_2/5%CO_2) was employed to investigate whether Gal-3 could mediate Th2 cells to promote proliferation of PASMCs. The purified $CD4^+$T cells were induced into Th2 cells, and then treated with Gal-3 over-expression (Fig. 4A). The findings presented that restoration of Gal-3 could promote Th2 cells to secret IL-4 and IL-5 (Fig. 4B), while no significant differences were found in the IL-13 expression. Interestingly, compared with the Th2 cells without treatment or Th2 cells with blocked IL-4 and IL-5 through neutralization, Th2 cells with elevated Gal-3 presented with markedly promoted growth of PASMCs (Fig. 4C), which was further verified by immunofluorescence assay (Fig. 4D-E). The above results demonstrated that Gal-3 promoted proliferation of PASMCs by activating the immune response to participate in the occurrence and development of PAH.

3.5. Adoptive transfer of CD4 + T cells promotes the progression of CHD-PAH in mice with Gal-3 knockdown

After uncovering that Gal-3 contributes to the facilitation of PASMC proliferation, we aimed to explore the effects of adoptive transfer of $CD4^+$T cells on CHD-PAH. As shown in Fig. 5A–B, CHD-PAH mice

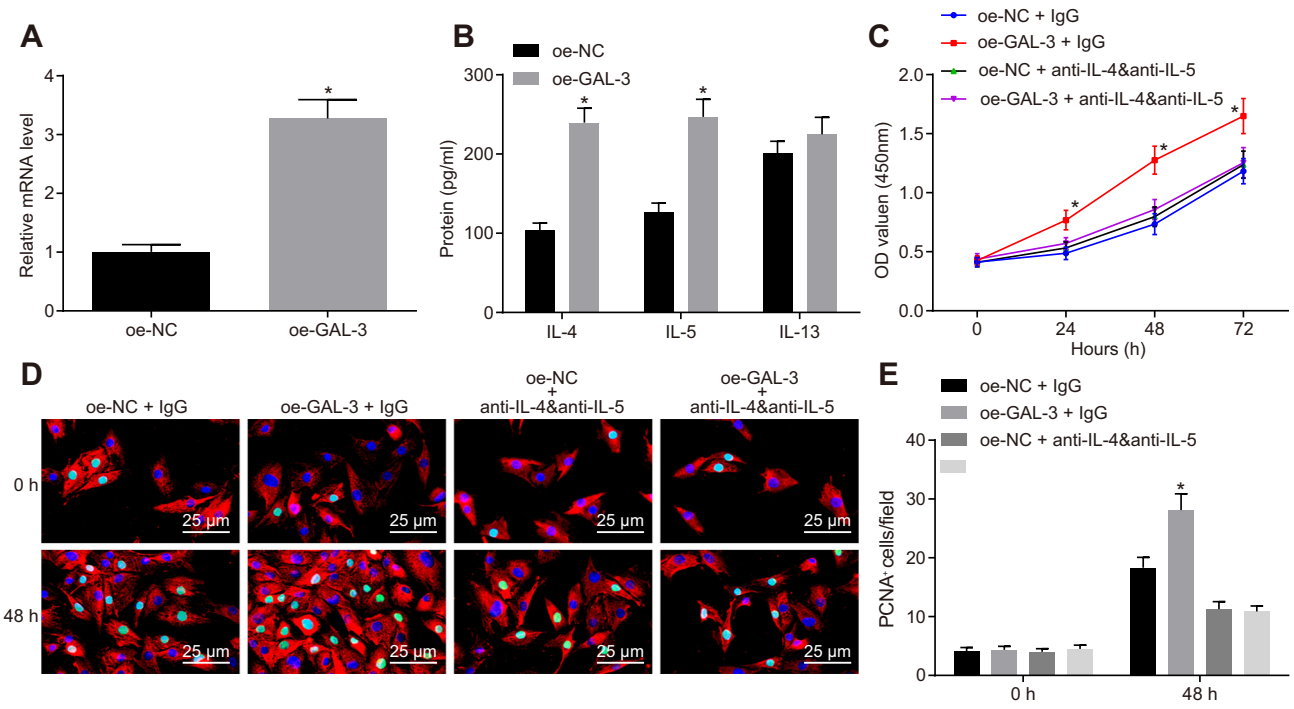

Fig. 4. Gal-3 promotes proliferation of PASMCs *via* activation of the immune response. A, Gal-3 expression in Th2 cells determined using RT-qPCR (**$p < 0.01$ *vs.* the oe-NC group [Th2 cells treated with oe-NC plasmids]. n = 3. Comparisons were analyzed using non-paired *t*-test). B, Levels of IL-4, IL-5, and IL-13 determined using ELISA (**$p < 0.01$ *vs.* the oe-NC group [Th2 cells treated with oe-NC plasmids]. The experiment was repeated 3 times, and comparisons were analyzed using non-paired *t*-test). C, Growth of PASMCs detected using CCK-8 (*$p < 0.05$, **$p < 0.01$ *vs.* the oe-NC + IgG group [Th2 cells treated with oe-NC and IgG plasmids]. The experiment was repeated 3 times, and comparisons at different point times were analyzed using repeated measures ANOVA [Tukey's *post hoc* test]). D, Proliferation of PASMCs detected using immunofluorescence assay (×400, PCNA [green], SMA [red], DAPI [blue]). E, Quantitative statistics for figure D (*$p < 0.05$, *vs.* the oe-NC + IgG group (Th2 cells treated with oe-NC and IgG plasmids). The experiment was repeated 3 times, and comparisons at different point times were analyzed using repeated measures ANOVA [Tukey's *post hoc* test]). Measurement data were depicted as mean ± standard deviation. (For interpretation of the references to colour in this figure legend, the reader is referred to the web version of this article.)

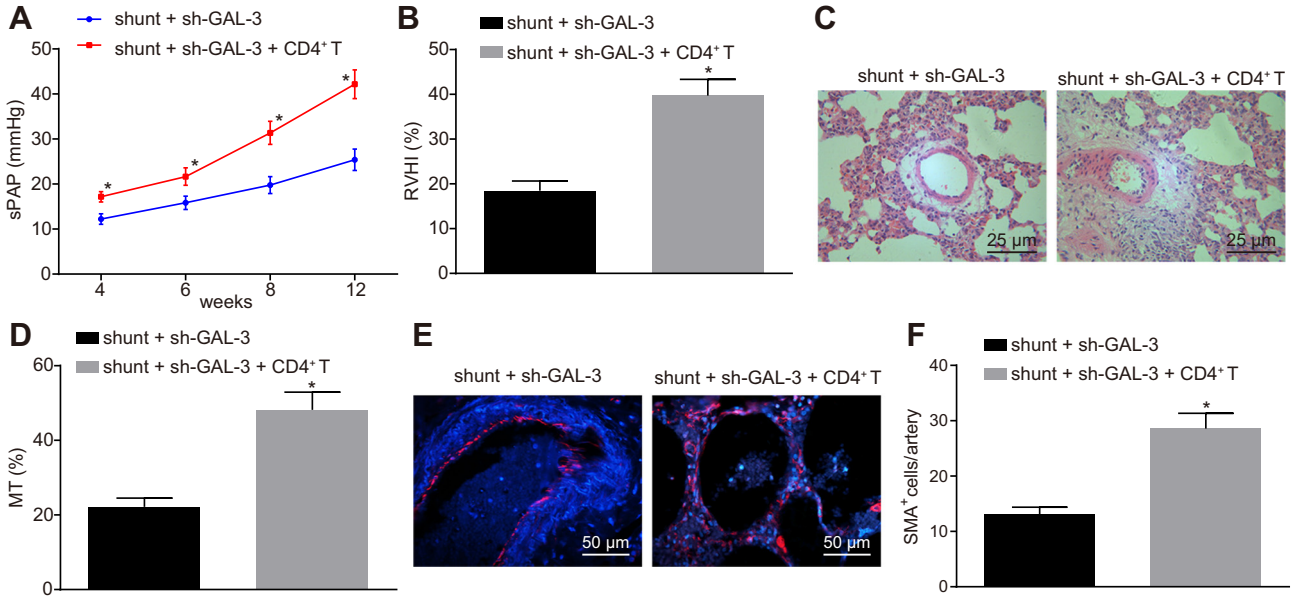

Fig. 5. Adoptive transfer of $CD4^+$T cells promotes the progression of CHD-PAH in mice with Gal-3 knockdown. A, sPAP of mice after treated with Gal-3 knockdown and $CD4^+$T cells. B, RVHI of mice at the 12th week after treated with Gal-3 knockdown and $CD4^+$T cells. C, Pulmonary vascular remodeling after treated with Gal-3 knockdown and $CD4^+$T cells observed using HE staining (×400). D, MT of pulmonary vascular wall at the 12th week in mice after treated with Gal-3 knockdown and $CD4^+$T cells. E, Immunofluorescence staining of α-SMA in lung tissue sections after treated with Gal-3 knockdown and $CD4^+$T cells (×200). H, SMCs in pulmonary artery after treated with Gal-3 knockdown and $CD4^+$T cells. *$p < 0.05$ *vs.* the shunt + sh-GAL-3 group (CHD-PAH mouse models treated with Gal-3 knockdown). Data were depicted as mean ± standard deviation. Comparisons between two groups were analyzed using non-paired *t*-test, and comparisons at different point times were analyzed using repeated measures ANOVA (Tukey's *post hoc* test). n = 12.

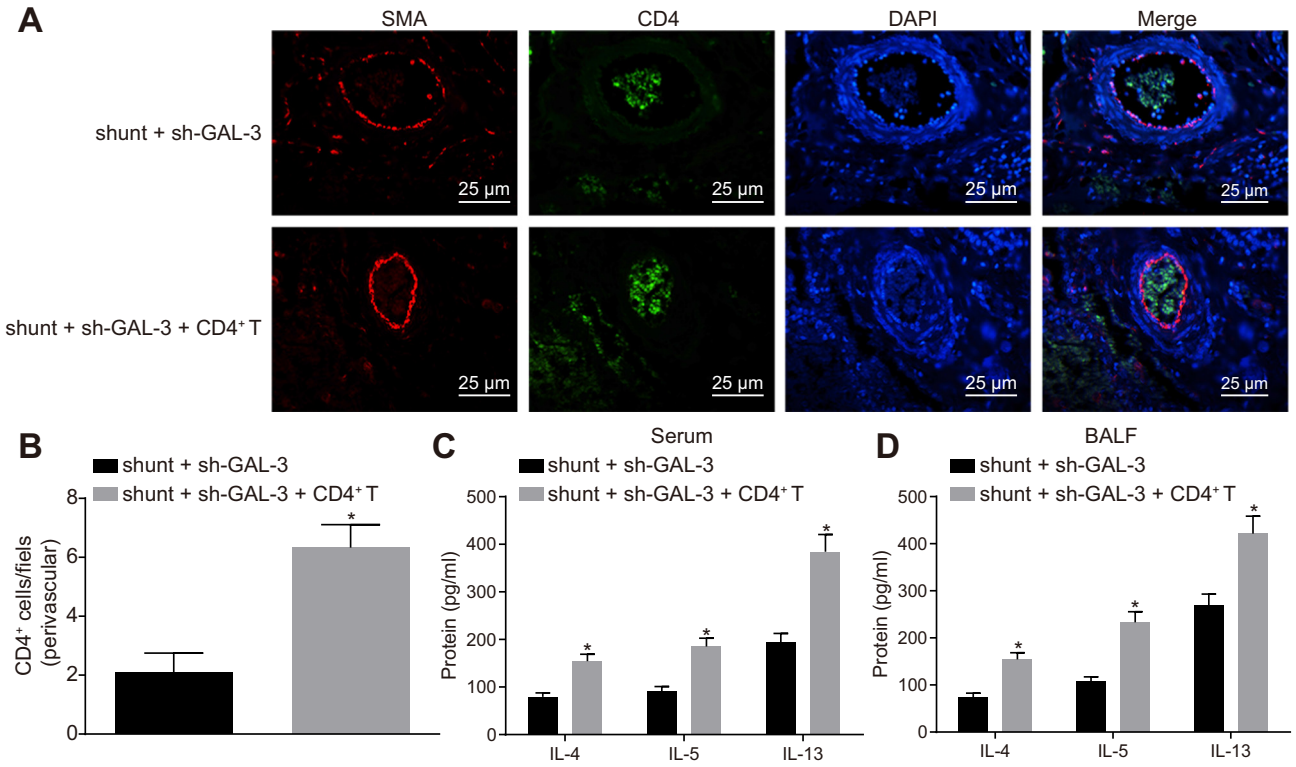

Fig. 6. Adoptive transfer of CD4$^+$T cells promotes CD4$^+$T cell perivascular infiltration in mice with Gal-3 knockdown. A, Immunofluorescence staining for lung tissue sections (×400, α-SMA [red], CD4 [red], DAPI [blue]). B, The number of perivascular CD4$^+$T cells in lung tissues. C, Levels of IL-4, IL-5, and IL-13 in the serum after treated with Gal-3 knockdown and CD4$^+$T cells using ELISA. D, Levels of IL-4, IL-5, and IL-13 in the BALF after treated with Gal-3 knockdown and CD4$^+$T cells using ELISA. *$p < 0.05$ *vs.* the shunt + sh-GAL-3 group (CHD-PAH mouse models treated with Gal-3 knockdown). Comparisons between two groups were analyzed using non-paired *t*-test. (For interpretation of the references to colour in this figure legend, the reader is referred to the web version of this article.)

treated with Gal-3 knockdown and CD4$^+$T presented with elevated sPAP and RVHI when compared with the CHD-PAH mice treated with Gal-3 knockdown. CD4$^+$T increased MT of pulmonary vascular wall and VSMCs in the CHD-PAH mice treated with Gal-3 knockdown (Fig. 5C–D), which was further verified by immunofluorescence assay (Fig. 5E–F). Similarly, compared with the CHD-PAH mice treated with Gal-3 knockdown, CHD-PAH mice treated with Gal-3 knockdown and CD4$^+$T exhibited increased CD4$^+$T cell perivascular infiltration in lung tissues and secretion of Th2 cytokine from serum and BALF of mice (Fig. 6A–D). Taken together, these findings revealed that Gal-3 depletion could inhibit Th2 activation and reduce pulmonary remodeling to suppress the progression of CHD-PAH.

4. Discussion

PAH is a highly prevalent complication of the left-to-right shunt type, which is common in CHD [6]. PAH is a severe disease characterized by vascular proliferation and remodeling of the pulmonary arteries, which leads to gradual elevation in pulmonary vascular resistance and right ventricular failure and ultimately, death [28]. Despite various advances in treatment regimens, PAH still remains to be incurable with high morbidity and fatality rates [29]. Thus, it is necessary to identify novel treatment strategies against PAH in patients suffering from CHD. The current study was performed aiming to examine the facilitating role of Gal-3 in PAH to elucidate the potential mechanism associated with immunomodulation. The key observations of the current study revealed that Gal-3 could expedite the progression of PAH in patients with CHD *via* activation of the immune response.

Firstly, we uncovered that Gal-3 was highly expressed in CHD-PAH patients. Gal-3 belongs to the β-galactoside binding lectin family that is widely found in multiple types of cells and tissues [30]. They share similar structures and play important roles in the inflammatory process, and Gal-1 has further been reported to participate in the occurrence of PAH [31]. Another study revealed that the expression of Gal-3 is correlated to several indices of RV function and morphology in PAH [32]. Similarly, Gal-3 levels were previously demonstrated to be associated with the clinical features and outcomes in patients with CHD, and were further up-regulated in patients with CHD [15]. Luo et al. indicated that Gal-3 levels are also significantly elevated in hypoxia-induced PAH patients [13], which is consistent with the findings of the current study.

Additionally, our findings confirmed that that Gal-3 elevated the levels of IL-4, IL-5, and IL-13, suggesting that Gal-3 activates the immune response in CHD-PAH. The Th2 cell-derived cytokines, including IL-4, IL-5, and IL-13, are capable of functioning in several cells types to induce pulmonary inflammation [33]. It is reported that IL-4 and IL-13 exert great effects on the activation of signaling pathway, which modulates immunologic response [34]. Moreover, galectins are known to play key roles in the immune response or inflammation, serving as novel therapy targets for multiple diseases, such as chronic inflammation [35]. Gal-3 has been further demonstrated to contribute to inflammation and fibrosis, which are known factors that participate in the progression of pulmonary arterial remodeling in PAH [36]. Additionally, adoptive transfer of CD4$^+$T cells was found to promote CD4$^+$T cell perivascular infiltration and the progression of CHD-PAH in mice with Gal-3 knockdown. Immune and inflammatory reactions can certainly influence PAH development, and increase the perivascular amount of helper T cells (CD4) in vessels of idiopathic PAH lungs [37]. In addition, another study indicated that Gal-3 may be significantly important in the regulation of Th2 differentiation [38]. More importantly, inflammation is believed to function as a key driver of PAH and some cytokines and chemokines are associated with poor prognosis of patients with PAH, highlighting the protective property of anti-inflammatory intervention [39]. These evidences support that Gal-3 promotes immune response by activating Th2 cells and anti-

inflammatory drugs may serve as potential targets for PAH treatment.

In addition, the current study revealed that restoration of Gal-3 increased sPAP and RVHI, SMCs and MT of the pulmonary vascular wall and stimulated proliferation of PASMCs by activating the immune response, which indicated that silencing of Gal-3 suppresses the progression of CHD-related PAH. One of the characteristics of PAH is pulmonary artery remodeling, which leads to obstruction of the vessel lumen and formation of complex vascular lesions [40]. It has been found that the proliferation of PASMCs is highly important in the pathobiology of PAH [4]. Gal-3 is implicated in some processes of pathology and physiology, such as immune responses, which are harmful to cardiac remodeling [12]. Furthermore, Gal-3 was indicated to serve as a potential target for RV remodeling in PAH [32]. Meanwhile, a previous study proved that Gal-3 knockdown relieves HPASMCs phenotype changing, and inhibits pulmonary vascular remodeling in PAH [13]. The progression of PAH is complicated with the promotion of proliferation and migration of PASMCs, which was demonstrated to be suppressed through inhibition of Gal-3 [41]. Additionally, it was previously confirmed that depletion of Gal-3 serves as a therapeutic biomarker for hypoxia-induced PAH treatment [14]. The abovementioned findings suggest that Gal-3 inhibition can suppress the progression of CHD-PAH *via* activation of the immune response. The implication of the AKT signaling pathway in the occurrence of PAH has been previously noted and reported [25–27], which encouraged us to determine the role of the AKT signaling pathway in CHD-PAH, results of which indicated that the presence of sh-GAL3 led to decreased levels of p-AKT; however, the detailed regulatory mechanism still needs further investigation.

In conclusion, the current study evidenced that Gal-3 could aggravate PAH in patients with CHD by activating the immune response, suggesting that silencing of Gal-3 may inhibit the progression and development of CHD-PAH. Thereby, it can be inferred that Gal-3 may serve as a novel therapeutic target of the treatment of PAH in patients with CHD. However, the experiments with regard to specific smooth muscle knockout of Gal-3 are required in the future to further understand the underlying mechanisms of Gal-3 in CHD-PAH.

Author contribution

Qiang Shen and Qingsong Liang designed the study. Wei Chen and Jun Liu collated the data, carried out data analyses and produced the initial draft of the manuscript. Qiang Shen, Wei Chen, Jun Liu and Qingsong Liang contributed to drafting the manuscript. All authors contributed to the revision and approved the final submitted manuscript.

Declaration of Competing Interest

The authors report no conflict of interest.

Acknowledgments

We acknowledge and appreciate our colleagues for their valuable efforts and comments on this paper.

References

[1] P. Steele, G. Strange, J. Wlodarczyk, B. Dalton, S. Stewart, E. Gabbay, et al., Hemodynamics in pulmonary arterial hypertension (pah): do they explain long-term clinical outcomes with pah-specific therapy? BMC Cardiovasc. Disord. 10 (2010) 9.

[2] I.R. Preston, K.E. Roberts, D.P. Miller, G.P. Sen, M. Selej, W.W. Benton, et al., Effect of warfarin treatment on survival of patients with pulmonary arterial hypertension (pah) in the registry to evaluate early and long-term pah disease management (reveal), Circulation 132 (2015) 2403–2411.

[3] H. Lee, J.C. Lee, J.H. Kwon, K.C. Kim, M.S. Cho, Y.S. Yang, et al., The effect of umbilical cord blood derived mesenchymal stem cells in monocrotaline-induced pulmonary artery hypertension rats, J. Korean Med. Sci. 30 (2015) 576–585.

[4] N. Zhu, X. Zhao, Y. Xiang, S. Ye, J. Huang, W. Hu, et al., Thymoquinone attenuates monocrotaline-induced pulmonary artery hypertension via inhibiting pulmonary arterial remodeling in rats, Int. J. Cardiol. 221 (2016) 587–596.

[5] L.J. Rubin, N. Galie, F. Grimminger, E. Grunig, M. Humbert, Z.C. Jing, et al., Riociguat for the treatment of pulmonary arterial hypertension: a long-term extension study (patent-2), Eur. Respir. J. 45 (2015) 1303–1313.

[6] B.S. Lowe, J. Therrien, R. Ionescu-Ittu, L. Pilote, G. Martucci, A.J. Marelli, Diagnosis of pulmonary hypertension in the congenital heart disease adult population impact on outcomes, J. Am. Coll. Cardiol. 58 (2011) 538–546.

[7] G.P. Diller, M.A. Gatzoulis, Pulmonary vascular disease in adults with congenital heart disease, Circulation 115 (2007) 1039–1050.

[8] M. Zhang, Z. Feng, R. Huang, C. Sun, Z. Xu, Characteristics of pulmonary vascular remodeling in a novel model of shunt-associated pulmonary arterial hypertension, Med. Sci. Monit. 24 (2018) 1624–1632.

[9] G. Giannakoulas, M.A. Gatzoulis, Pulmonary arterial hypertension in congenital heart disease: current perspectives and future challenges, Hell. J. Cardiol. (2016) (pii: S1109-9666(16)30144-0).

[10] L. Calvier, E. Martinez-Martinez, M. Miana, V. Cachofeiro, E. Rousseau, J.R. Sadaba, et al., The impact of galectin-3 inhibition on aldosterone-induced cardiac and renal injuries, JACC Heart Fail. 3 (2015) 59–67.

[11] L. Calvier, M. Miana, P. Reboul, V. Cachofeiro, E. Martinez-Martinez, R.A. de Boer, et al., Galectin-3 mediates aldosterone-induced vascular fibrosis, Arterioscler. Thromb. Vasc. Biol. 33 (2013) 67–75.

[12] L. Calvier, E. Legchenko, L. Grimm, H. Sallmon, A. Hatch, B.D. Plouffe, et al., Galectin-3 and aldosterone as potential tandem biomarkers in pulmonary arterial hypertension, Heart 102 (2016) 390–396.

[13] H. Luo, B. Liu, L. Zhao, J. He, T. Li, L. Zha, et al., Galectin-3 mediates pulmonary vascular remodeling in hypoxia-induced pulmonary arterial hypertension, J. Am. Soc. Hypertens. 11 (2017) 673–683 e673.

[14] M. Hao, M. Li, W. Li, Galectin-3 inhibition ameliorates hypoxia-induced pulmonary artery hypertension, Mol. Med. Rep. 15 (2017) 160–168.

[15] V.J.M. Baggen, A.E. van den Bosch, J.A. Eindhoven, M.E. Menting, M. Witsenburg, J. Cuypers, et al., Prognostic value of galectin-3 in adults with congenital heart disease, Heart 104 (2018) 394–400.

[16] G. Wang, X. Liu, L. Meng, S. Liu, L. Wang, J. Li, et al., Up-regulated lipocalin-2 in pulmonary hypertension involving in pulmonary artery smc resistance to apoptosis, Int. J. Biol. Sci. 10 (2014) 798–806.

[17] Y. Xiao, D. Gong, W. Wang, Soluble jagged1 inhibits pulmonary hypertension by attenuating notch signaling, Arterioscler. Thromb. Vasc. Biol. 33 (2013) 2733–2739.

[18] M. Kataoka, T. Kawakami, Y. Tamura, H. Yoshino, T. Satoh, T. Tanabe, et al., Gene transfer therapy by either type 1 or type 2 adeno-associated virus expressing human prostaglandin i2 synthase gene is effective for treatment of pulmonary arterial hypertension, J. Cardiovasc. Pharmacol. Ther. 18 (2013) 54–59.

[19] M. Shi, G. Shi, J. Tang, D. Kong, Y. Bao, B. Xiao, et al., Myeloid-derived suppressor cell function is diminished in aspirin-triggered allergic airway hyperresponsiveness in mice, J. Allergy Clin. Immunol. 134 (e1116) (2014) 1163–1174.

[20] W. Shi, C. Zhai, W. Feng, J. Wang, Y. Zhu, S. Li, et al., Resveratrol inhibits monocrotaline-induced pulmonary arterial remodeling by suppression of sphk1-mediated nf-kappab activation, Life Sci. 210 (2018) 140–149.

[21] G. Chen, S. Zuo, J. Tang, C. Zuo, D. Jia, Q. Liu, et al., Inhibition of crth2-mediated th2 activation attenuates pulmonary hypertension in mice, J. Exp. Med. 215 (2018) 2175–2195.

[22] Z. Li, Y. Zhang, Z. Liu, X. Wu, Y. Zheng, Z. Tao, et al., Ecm1 controls t(h)2 cell egress from lymph nodes through re-expression of s1p(1), Nat. Immunol. 12 (2011) 178–185.

[23] H.R. Jiang, Z. Al Rasebi, E. Mensah-Brown, A. Shahin, D. Xu, C.S. Goodyear, et al., Galectin-3 deficiency reduces the severity of experimental autoimmune encephalomyelitis, J. Immunol. 182 (2009) 1167–1173.

[24] M. Dandel, G. Wallukat, A. Englert, R. Hetzer, Immunoadsorption therapy for dilated cardiomyopathy and pulmonary arterial hypertension, Atheroscler. Suppl. 14 (2013) 203–211.

[25] J. Dai, Q. Zhou, J. Chen, M.L. Rexius-Hall, J. Rehman, G. Zhou, Alpha-enolase regulates the malignant phenotype of pulmonary artery smooth muscle cells via the ampk-akt pathway, Nat. Commun. 9 (2018) 3850.

[26] C.C. Cheng, P.L. Chi, M.C. Shen, C.W. Shu, S.R. Wann, C.P. Liu, et al., Caffeic acid phenethyl ester rescues pulmonary arterial hypertension through the inhibition of akt/erk-dependent pdgf/hif-1alpha in vitro and in vivo, Int. J. Mol. Sci. 20 (2019).

[27] A.F. Silva, G. Faria-Costa, F. Sousa-Nunes, M.F. Santos, M.J. Ferreira-Pinto, D. Duarte, et al., Anti-remodeling effects of xanthohumol-fortified beer in pulmonary arterial hypertension mediated by erk and akt inhibition, Nutrients 11 (2019).

[28] M. Humbert, O. Sitbon, A. Chaouat, M. Bertocchi, G. Habib, V. Gressin, et al., Survival in patients with idiopathic, familial, and anorexigen-associated pulmonary arterial hypertension in the modern management era, Circulation 122 (2010) 156–163.

[29] W.T. Lee, Y. Ling, K.K. Sheares, J. Pepke-Zaba, A.J. Peacock, M.K. Johnson, Predicting survival in pulmonary arterial hypertension in the Uk, Eur. Respir. J. 40 (2012) 604–611.

[30] J.P. Cerliani, A.G. Blidner, M.A. Toscano, D.O. Croci, G.A. Rabinovich, Translating the 'sugar code' into immune and vascular signaling programs, Trends Biochem. Sci. 42 (2017) 255–273.

[31] I.M. Seropian, G.E. Gonzalez, S.M. Maller, D.H. Berrocal, A. Abbate, G.A. Rabinovich, Galectin-1 as an emerging mediator of cardiovascular inflammation: mechanisms and therapeutic opportunities, Mediat. Inflamm. 2018 (2018) 8696543.

[32] B.E. Fenster, L. Lasalvia, J.D. Schroeder, J. Smyser, L.J. Silveira, J.K. Buckner, et al.,

Galectin-3 levels are associated with right ventricular functional and morphologic changes in pulmonary arterial hypertension, Heart Vessel. 31 (2016) 939–946.
[33] P. Dasgupta, S.P. Chapoval, E.P. Smith, A.D. Keegan, Transfer of in vivo primed transgenic t cells supports allergic lung inflammation and fizz1 and ym1 production in an il-4ralpha and stat6 dependent manner, BMC Immunol. 12 (2011) 60.
[34] R. Kumar, C. Mickael, J. Chabon, L. Gebreab, A. Rutebemberwa, A.R. Garcia, et al., The causal role of il-4 and il-13 in schistosoma mansoni pulmonary hypertension, Am. J. Respir. Crit. Care Med. 192 (2015) 998–1008.
[35] G.A. Rabinovich, F.T. Liu, M. Hirashima, A. Anderson, An emerging role for galectins in tuning the immune response: lessons from experimental models of inflammatory disease, autoimmunity and cancer, Scand. J. Immunol. 66 (2007) 143–158.
[36] X. Wang, Y. Wang, J. Zhang, X. Guan, M. Chen, Y. Li, et al., Galectin-3 contributes to vascular fibrosis in monocrotaline-induced pulmonary arterial hypertension rat model, J. Biochem. Mol. Toxicol. 31 (2017).
[37] R. Savai, S.S. Pullamsetti, J. Kolbe, E. Bieniek, R. Voswinckel, L. Fink, et al., Immune and inflammatory cell involvement in the pathology of idiopathic pulmonary arterial hypertension, Am. J. Respir. Crit. Care Med. 186 (2012) 897–908.
[38] A. Fermin Lee, H.Y. Chen, L. Wan, S.Y. Wu, J.S. Yu, A.C. Huang, et al., Galectin-3 modulates th17 responses by regulating dendritic cell cytokines, Am. J. Pathol. 183 (2013) 1209–1222.
[39] P. Ghataorhe, C.J. Rhodes, L. Harbaum, M. Attard, J. Wharton, M.R. Wilkins, Pulmonary arterial hypertension - progress in understanding the disease and prioritizing strategies for drug development, J. Intern. Med. 282 (2017) 129–141.
[40] J.A. Leopold, B.A. Maron, Molecular mechanisms of pulmonary vascular remodeling in pulmonary arterial hypertension, Int. J. Mol. Sci. 17 (2016).
[41] S. Guo, Z. Feng, Galectin-3 mediates the effect of pdgf on pulmonary arterial hypertension, Int. J. Clin. Exp. Med. 8 (2015) 15302–15307.